Journal of Coastal Research	SI	38	106–124	West Palm Beach, Florida	Fall 2003

Mapping Shoreline Change Using Digital Orthophotogrammetry on Maui, Hawaii

Charles Fletcher†, John Rooney†, Mathew Barbee†, Siang-Chyn Lim†, Bruce Richmond‡

†Department of Geology and Geophysics
University of Hawaii
1680 East West Road
Honolulu, HI 96822

‡U.S. Geological Survey
Western Region Coastal and Marine Geology Program
345 Middlefield Road
Menlo Park, CA 94025

ABSTRACT

FLETCHER, C.; ROONEY, J.; BARBEE, M.; LIM, S.-C., and RICHMOND, B., 2004. Mapping shoreline change using digital orthophotogrammetry on Maui, Hawaii. *Journal of Coastal Research,* SI(38), 106–124. West Palm Beach (Florida), ISSN 0749-0208.

Digital, aerial orthophotomosaics with 0.5–3.0 m horizontal accuracy, used with NOAA topographic maps (T-sheets), document past shoreline positions on Maui Island, Hawaii. Outliers in the shoreline position database are determined using a least median of squares regression. Least squares linear regression of the reweighted data (outliers excluded) is used to determine a shoreline trend termed the reweighted linear squares (RLS). To determine the annual erosion hazard rate (AEHR) for use by shoreline managers the RLS data is smoothed in the longshore direction using a weighted moving average five transects wide with the smoothed rate applied to the center transect. Weightings within each five transect group are 1,3,5,3,1. AEHR's (smoothed RLS values) are plotted on a 1:3000 map series for use by shoreline managers and planners. These maps are displayed on the web for public reference at http://www.co.maui.hi.us/departments/Planning/erosion.htm. An end-point rate of change is also calculated using the earliest T-sheet and the latest collected shoreline (1997 or 2002). The resulting database consists of 3565 separate erosion rates spaced every 20 m along 90 km of sandy shoreline.

Three regions are analyzed: Kihei, West Maui, and North Shore coasts. The Kihei Coast has an average AEHR of about 0.3 m/yr, an end point rate (EPR) of 0.2 m/yr, 2.8 km of beach loss and 19 percent beach narrowing in the period 1949–1997. Over the same period the West Maui coast has an average AEHR of about 0.2 m/yr, an average EPR of about 0.2 m/yr, about 4.5 km of beach loss and 25 percent beach narrowing. The North Shore has an average AEHR of about 0.4 m/yr, an average EPR of about 0.3 m/yr, 0.8 km of beach loss and 15 percent beach narrowing.

The mean, island-wide EPR of eroding shorelines is 0.24 m/yr and the average AEHR of eroding shorelines is about 0.3 m/yr. The overall shoreline change rate, erosion and accretion included, as measured using the unsmoothed RLS technique is 0.21 m/yr. Island wide changes in beach width show a 19 percent decrease over the period 1949/1950 to 1997/2002. Island-wide, about 8 km of dry beach has been lost since 1949 (i.e., high water against hard engineering structures and natural rock substrate).

ADDITIONAL INDEX WORDS: *Coastal erosion, shoreline change, photogrammetry, setbacks, coastal management, coastal geology.*

INTRODUCTION

Beaches are fundamentally important to the Hawaiian economy, the marine ecosystem, the culture, and the lifestyle of island residents. Tourism provides over 60 percent of the jobs in the state and beaches are a major reason why visitors come to the islands.

Coastal erosion is a source of widespread concern because of threats to abutting private lands and loss of beach resources. Estimates of beach loss related to shoreline armoring on chronically eroding lands (Figure 1) have entered the public dialogue on resource management and protection (FLETCHER *et al.,* 1997; FLETCHER and LEMMO, 1999).

In its role as a resource management and planning agency, the Maui County Planning Department requested that the University of Hawaii conduct a study of coastal erosion rates and patterns along the entire sandy shoreline of Maui Island. Here we report on the methodology used in that study and present the resulting regional-scale statistics describing historical patterns of shoreline movement.

PHYSICAL SETTING

White sand beaches in Hawaii are composed of variable percentages of coralline and calcareous algae, coral, mollusk, and echinoderm fragments (HARNEY *et al.,* 1999). Although originating as the sedimentary product of reef system metabolism, on many low-lying Hawaiian shores the greatest

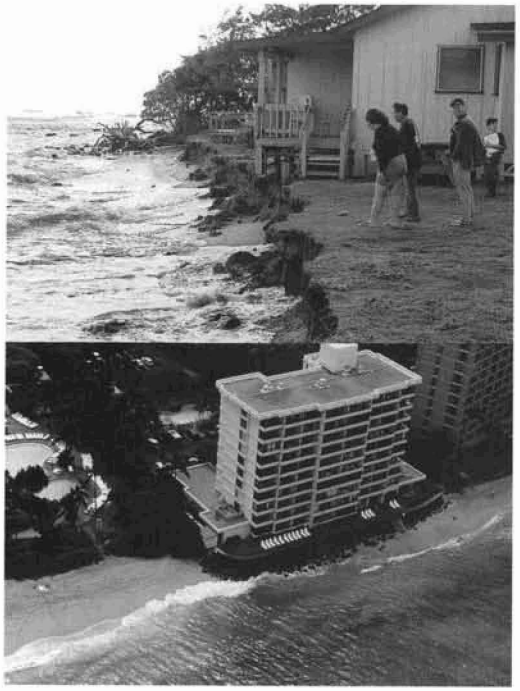

Figure 1. Top—Kauai. Chronic erosion threatens homes on all Hawaiian Islands. Bottom—Maui. Historically, shoreline hardening has been the most frequently used tool to manage chronic erosion.

Figure 2. Vertical aerial photograph of coastal home. Low-lying coastal plains of many Hawaiian beaches are composed of carbonate sand deposited under a higher than present sea level ca. 3000 BP (CALHOUN and FLETCHER, 1995; FLETCHER and JONES, 1996; GROSSMAN and FLETCHER, 1998; HARNEY *et al.*, 1999). The region immediately offshore of most beaches is barren limestone (fossil reef) with localized sand deposits that may or may not be active in the littoral sediment budget. Natural sand nourishment on sand deficient beaches occurs when coastal plain sands are released by erosion. Sand impoundment behind seawalls removes this principal source of sand to the beaches.

accumulation of stored sands are found on formerly accreting coastal plains associated with a late Holocene fall of sea level ca. 2000 BP to pre-modern era. Radiocarbon dates of carbonate sand from coastal plain, beach, and reef environments document late middle to late Holocene ages and a notable lack of modern sands (CALHOUN and FLETCHER, 1995; FLETCHER and JONES, 1996; GROSSMAN and FLETCHER, 1998; HARNEY *et al.*, 1999). Maui's beaches (and other Hawaiian beaches) then, are the exposed erosional edge of these sand-rich coastal plain deposits (Figure 2). Although beach dynamics dominated by longshore transport characterize Hawaiian beaches (NORCROSS *et al.*, 2002; DAIL *et al.*, 2000) long-term sediment budgets experiencing chronic deficits rely upon erosional release of sand from the adjacent coastal plain. In many cases, chronic deficits are widely believed to be the result of historical sand mining and other examples of poor sand management.

The Maui wave climate has a distinct seasonal signal that is typical of all Hawaiian Islands. The general Hawaiian wave climate consists of four types of waves: northeast tradewind waves, North Pacific swell, south swell, and Kona storm waves (Figure 3). Tsunami and hurricane waves, both of which are potentially erosive, are also known to impinge on the Maui shoreline from time to time.

The winter months of October through March are dominated by high winter swell generated by severe storms in the North Pacific and mid-latitude low pressure areas. Typical heights are 1.5 to 6 m with periods of 12 to 20 s. North swell are incident to shores with a northern exposure.

South swell is generated by storms in the south-

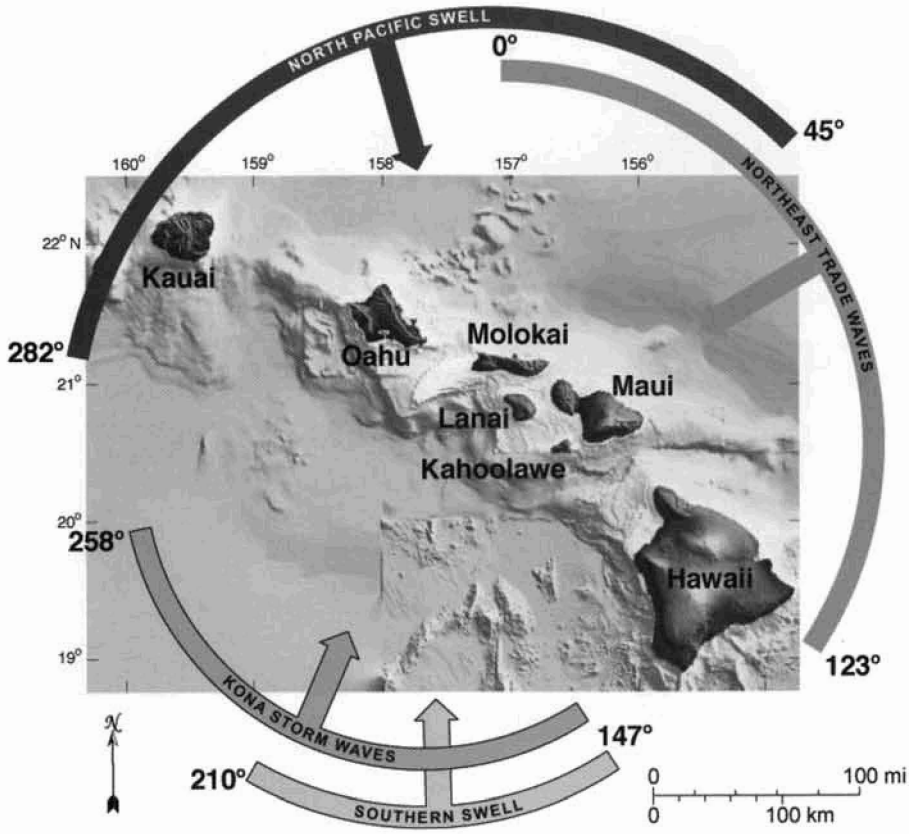

Figure 3. Waves of the Hawaiian Islands.

ern hemisphere over the months of April to October. These waves tend to be long and low with heights of <1 to 3 m and periods of 12 to 20 s. High summer southern swells influence sand transport along south and west shores. Commonly, refraction of northern and southern wave types influences coastal processes on adjacent windward and leeward shores.

Trade winds generate local seas <1 to 3 m in height and 6 to 8 s in period over 80 percent of the time between April and September. These waves are incident to northeasterly and easterly shores and run oblique to shores on other reaches of the island. Trade wind waves cause changes in beach morphology related to short duration increases in wind speed that raise wave energy. Such changes tend not to have a strong seasonal signal but are instead episodic over the April to September period.

Kona waves are generated by intense winds associated with local storms originating from the south in most cases. In a recent study, ROONEY (2001) proposes that the Pacific Decadal Oscillation (PDO) modulates the occurrence of southerly or Kona storms which are high intensity, short duration frontal systems that drive shoreline change on exposed beaches. Kona's tend to occur with greater frequency during negative phases of the PDO. Hence, shoreline change patterns may reflect periods of enhanced storminess on the decadal scale in the history of some beaches. Kona waves typically range from 3 to 6 m in height with periods of 6 to 10 s.

A fringing reef abuts many Maui beaches serving to modulate and dissipate wave energy and provide some storage of sand related to active coastal processes. Highly variable reef topography exerts localized control over shoreline processes by forcing the convergence and divergence of wave energy on the adjacent beach.

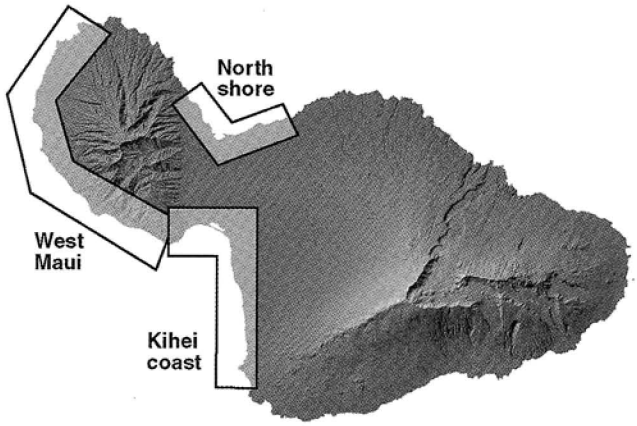

Figure 4. The study area consists of three coastal segments characterized by sandy beaches: Kihei Coast, West Maui, and North Shore; other coastal regions of Maui are characterized by steep rocky shorelines and cliffs.

METHODOLOGY

Maui's sandy shoreline occurs in three geographic regions named the Kihei Coast, West Maui, and North Shore (Figure 4). A combination of historical NOAA NOS topographic maps (T-sheets), hydrographic charts (H-sheets), and large-scale vertical aerial photographs were used in this study to determine historical shoreline positions and calculate long-term erosion rates (ANDERS and BYRNES, 1991). Between six and nine historical shoreline positions were defined across approximately 90 km of sandy coast and rates of shoreline movement calculated every 20 m in the alongshore direction for a total of approximately 3565 rate determinations. A methodology was designed to provide high-resolution rates of long-term shoreline change that are generally statistically significant and free of the influence of storms, tsunami, and seasonally extreme positions.

Historical shorelines were produced using orthorectified, high resolution vertical aerial photographs and historical sheets and charts in a digital environment. This process is described in following sections. PCI Geomatics, Inc. (http://www.pcigeomatics.com/) photogrammetric modules were used for this task and employ US Geological Survey (http://www.usgs.gov/) digital elevation models and differential global positioning system (DGPS) surveys in the orthorectification process.

T-Sheets

Georectified digital files (.jpg and geotiff) of inked mylar T-sheets and H-sheets were provided for this project by the NOAA Coastal Services Center (http://www.csc.noaa.gov/). These maps, in scales of 1:2,500, 1:5,000, 1:10,000 and 1:20,000, carry the surveyed position of the contemporaneous high water mark as measured by plane table and alidade in the early 20th century.

Several workers have addressed the accuracy of T-sheets (Figure 5). CROWELL *et al.* (1991) determined that sheets at a scale of 1:20,000 carried a positional accuracy of ±8.9 m. In 1990, the National Academy of Sciences Committee on Coastal Erosion Zone Management (NAS, 1990) recommended the use of T-sheets in historical shoreline mapping. About T-sheets they said "This high accuracy makes them quite useful in delineating the land-water boundary and particularly for determining net changes over the long term." (p. 123). In 1993, CROWELL *et al.* reported that combinations of T-sheets and aerial photographs provide useful time series of shoreline positions and that the accuracy of such series was improved by the extension of the overall length of the study period as a result of using T-sheets. DANIELS and HUXFORD (2001) tested the position accuracy of T-sheets using differential GPS and derived an accuracy of ±3 m at 1:5,000, ±6 m at 1:10,000 and ±8 m at 1:20,000. National map accuracy standards (ELLIS, 1978) prescribe an accuracy of ±10.4

Figure 5. Portion of a 1912 1:20,000 T-sheet, West Maui coastal segment.

m for 1:20,000 T-sheets, ±8.5 m for 1:10,000 T-sheets, and ±3 m for 1:5,000 T-sheets.

We use on-screen digitizing to define a shoreline vector from the T-sheets. Because the Hawaiian shoreline is characterized by frequent basaltic headlands, these provide a convenient local test of T-sheet accuracy. Before accepting a T-sheet derived shoreline for analysis, we apply two qualitative accuracy tests. First, T-sheet triangulation stations marked on the maps are tested for position accuracy against modern orthorectified photomosaics. In most (nearly all) cases, surveyor's descriptions of triangulation stations allow their identification on modern orthophotomosaics. A misfit greater than national map accuracy standards between station coordinates as digitized from a T-sheet and station coordinates on an orthophotomosaic is grounds for rejection of the T-sheet shoreline. Secondly we test the goodness of fit of the shoreline around rocky headlands, outcrops and other promontories along the Maui coast by overlaying the digitized T-sheet shoreline vector on an orthophotomosaic.

Where appropriate and when a clear improvement in the accuracy of a shoreline can be achieved, a vector may be shifted to better fit the position of rocky features that are assumed not subject to erosion. Since the intent of the original survey was to map the high water mark on both sandy and rocky shorelines it is assumed this introduces no bias to the shoreline. In most cases the T-sheet shoreline matched rocky features, and mapped triangulation stations matched their modern position within National Map Accuracy Standards. Of 19 T-sheet shorelines used in this study, two (portions of the Makena/Big Beach and Olowalu map areas) were rejected based on these tests and 8 were shifted to better fit the position of rocky features on orthophotomosaics.

Shoreline Reference Feature

Early surveyors were trained in recognizing shoreline features representing the nonstorm high tidal wash of the waves. The resulting shoreline, the high water line, was placed on maps and charts largely to serve as an aid to navigation. However, in order to track historical shoreline

Figure 6. Left—North Kaanapali Beach, West Maui, 1997. Right—North Kaanapali Beach, West Maui, 1988. The low water position is used as the shoreline change reference feature. It is observed in most aerial photos of Hawaiian beaches whereas other features such as the high water line are not apparent due to the lack of debris in the water and the high reflectivity of carbonate sands in older historical photographs. Attempts to highlight the high water position on historical photos using contrast stretching and brightness controls on image processing software have repeatedly been unsuccessful.

movements we use the toe of the beach (BAUER and ALLEN, 1995) as the shoreline reference feature. The toe, or the base of the foreshore, represents the approximate position of mllw. Hence, the T-sheet shoreline (high tide) must be migrated to the contemporaneous low water position in order to reduce the positional uncertainty of our analysis (Figure 6).

We use the low water position as a shoreline reference feature for several reasons. Past studies of Hawaiian beaches reveal a strong geomorphic control related to alongshore, rather than cross-shore profile adjustment. EVERSOLE (2002), studying Kaanapali Beach in west Maui, found a nearly closed budget of seasonal longshore sand exchange between terminal ends of the beach with little offshore loss. NORCROSS *et al.* (2002) used Principal Component Analysis at Kailua Beach, Oahu and revealed two strong modes of profile variability. One mode was associated with the berm crest and the other with the offshore breaker zone. These two regions changed morphology in phase. That is, they increased in elevation and decreased in elevation simultaneously. This was interpreted to be the result of longshore sediment transport while the region of the lower foreshore and inner breaker zone remained stable. On a seasonal basis, the low water position acted as a stable pivot point that was relatively immune to geomorphic changes occurring on the seaward and landward portions of the profile. The stable behavior of the toe was observed on beaches reacting to seasonal, nonstorm wave influences.

The high visual reflectivity of Hawaiian white carbonate beaches tends to mask the visual prominence of other types of reference features such as the wet-dry line, the water line, and the high-water line, especially in historical aerial photos that are acquired as contact prints rather than higher resolution diapositives. Attempts to highlight high water indicators on historical photos using brightness and contrast controls on image processing software repeatedly failed. The vegetation line is cultivated on all developed beaches and does not represent the natural movement of the shoreline.

A high degree of water clarity and a typical lack of abundant flotsam in Hawaiian waters allow the delineation of the low water position during on-screen digitizing activities and prevents a clear delineation of a high water mark on historical photos. Hence, we use the low water position as a relatively stable natural feature that is readily obtained from historical materials and accurately reflects long-term sand volume changes (because it is an actual geomorphic feature) but does not introduce significant uncertainty associated with short-term morphodynamic processes.

T-Sheet Shoreline Migration

In order to compare the high water position on T-sheets to the low water position on aerial photos, it is necessary to know the natural offset between the two features on Maui beaches. Knowledge of this offset allows software operators to run a module that migrates the T-sheet high water position to a new position that replicates the contemporaneous position of low water. We choose to migrate the single T-sheet shoreline rather than migrate eight low water shorelines (from air photos) because it introduces the least error of the two options. To assess the offset, we use a five-year data set of semiannual beach profiles (GIBBS *et al.*, 2002; http://geopubs.wr.usgs.gov/open-file/of01–308/) to develop site-specific geometric models of the offset between the high water position and the low water position. Twenty-seven beaches on Maui have been profiled during winter and summer seasons over five years to obtain these offsets. The mean offset calculated over the entire profile time series at each beach is applied as a correction to the position of the T-sheet high water line. Where shoreline movement is calculated on beaches lacking profile data, an offset is used from the nearest appropriate site experiencing similar littoral processes.

Photomosaics

Producing historical shorelines from vertical aerial photography requires that a modern shoreline be defined. We contracted two sets of vertical aerial photos, staged to correspond with the work schedule of the analysis. Two sets of photographs were flown, a 1997 survey at a scale of 1:5,200 covering the Kihei and West Maui study sites and a 2002 set flown at 1:19,500 covering the North Shore region. The 1997 photos were only available as contact prints and so a large-scale was necessary to achieve the desired ground resolution of 0.3–0.5 m. The 2002 photos were available as color diapositives that achieved the desired resolution at a smaller scale.

Flight lines were shore parallel centered on the shoreline with a 60 percent overlap between adjacent frames. Ground control points (GCPs) were collected at prominent geographic and cultural features using DGPS within the area of the photos. GCPs were collected at sub-centimeter precision in three dimensions. Between two and six GCPs were collected for each frame. Color film prints from the 1997 survey were scanned at 500 dpi and color diapositives from the 2002 survey at 2000 dpi.

Orthorectification and photomosaicing were performed using PCI Geomatics Inc. Orthoengine module. Each study region was divided into map areas typically extending between three to seven photo frames in the alongshore direction. Within a single map area each photo is opened in Orthoengine and all GCPs defined. A lead photo for the area is identified and matched to the USGS digital elevation model (DEM) for the site using rectified coordinates. The photo is orthorectified using GCPs and the DEM (Figure 7). Root mean square (RMS) estimates of orthorectification accuracy are used in uncertainty determinations and typically range between 0.5 and 3.0 m. All frames in a map area are orthorectified in this manner and then mosaiced using operator-identified tie points that lie within the 20 to 60 percent overlap of adjacent frames. This produces a shore-parallel orthorectified photomosaic constituting the map area.

Historical Shorelines

The PCI Imageworks module is used to construct a vector of the low water position as projected in the photomosaic. Operators employ the same methodology to construct orthorectified photomosaics of historical aerial photos. Historical photos used in this study date from 1949, 1960, 1963, 1975, 1988, 1987 (used to define seasonal uncertainty, not as a shoreline), 1997, 2002. Historical photos are orthorectified using tie points (or pass points) from the modern era mosaic, original GCP locations where identified, and the USGS DEM. All vectors representing photographic shorelines and T-sheet shorelines are used in the calculation of shoreline change rates.

Extreme Event Shorelines

Hawaii experienced at least four major storms or periods of increased storm activity during our time series: Hurricane Dot in 1959, early 1960s Kona storms, 1982 Hurricane Iwa, and 1992 Hurricane Iniki. Damaging tsunamis hit the shoreline in 1946, and in the late 1950's and early 1960s. Overall, 25 Central Pacific hurricanes are known since 1950 and some 138 tropical cyclones have been identified over the period 1970–2000 (FLETCHER *et al.*, 2002). Because storms and tsunamis usually impact shorelines on one side of an island at a time, not all beaches experience all events, nor do they react similarly to every event. Indeed, because first hand accounts are sparse, it is impossible to know which historical shorelines

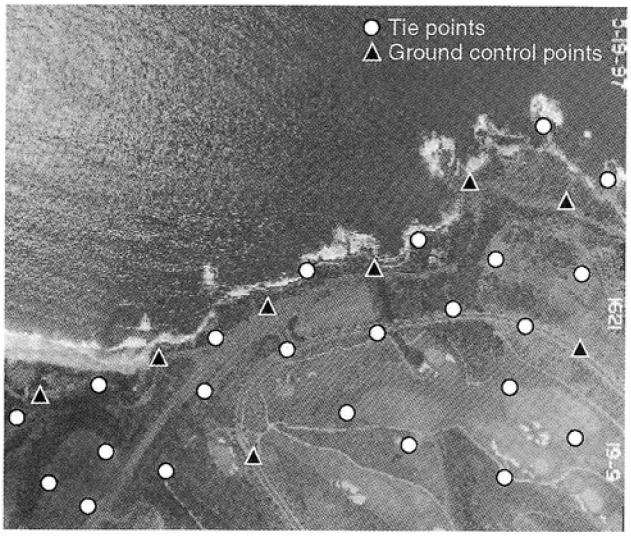

Figure 7. Orthorectification uses ground control points (GCPs, triangles) and tie points (circles) to correct modern images. GCPs provide elevation and position control and tie points are used to create seamless orthorectified photomosaics.

represent extreme event positions. We found that the storm history provided insufficient basis for eliminating extreme event shorelines *a priori.*

A further problem exists in the seasonality of beach morphodynamics in Hawaii. Historical shorelines may represent seasonal extremes in the annual cycle of a shoreline and as such are not desirable in the calculation of change rates. Further, southerly-facing shorelines tend to erode in the summer season and northerly-facing shores tend to erode in the winter. East and west-facing shores experience refracted swell from both south and north to varying degrees and will react accordingly, alternating between erosion and accretion on an intraseasonal basis. Hence, isolating true storm shorelines in Hawaii is problematic.

Extreme erosional shoreline positions and the period of accretion that typically follows can lead to erroneous calculation of a long-term shoreline trend (DOUGLAS and CROWELL, 2000). Therefore it is important that extreme shoreline positions be removed from any dataset attempting to determine a long-term trend. We address this problem with the application of the reweighted least squares method (ROUSSEEUW, 1990). This two-part technique uses a least median of squares (LMS) regression that identifies statistical outlier points in the time series at each transect. The LMS can identify up to 50 percent of the population of a random, independent, and unbiased dataset as outliers. Historical shorelines that are identified as outliers by LMS are considered storm shorelines or seasonal extremes and rejected from consideration in the line-fitting procedure. By visual inspection, care was given to ensure that any identification of a T-sheet shoreline as an outlier was not simply because of the temporal gap prior to the first photo shoreline (1949). The LMS technique was only applied to the calculation of an annual erosion hazard rate using linear regression. End-point rate calculations were always made using the earliest T-sheet or aerial photo and the 1997 or 2002 aerial photo. We perform the calculation to remove extreme event shorelines following the suggestion of DOUGLAS and CROWELL (2000) and HONEYCUTT *et al.* (2002). The trend of the resulting, reweighted (outlier points removed) dataset is determined using least squares regression.

Shoreline Change Rates

Change rates are calculated at shore normal transects spaced 20 m alongshore. Measurements of shoreline position are referenced to an arbitrary baseline located offshore of the beach. Because the baseline does not exactly mimic the meander of the shoreline, some transects will cross. These are edited to reduce confusion in the location of shoreline

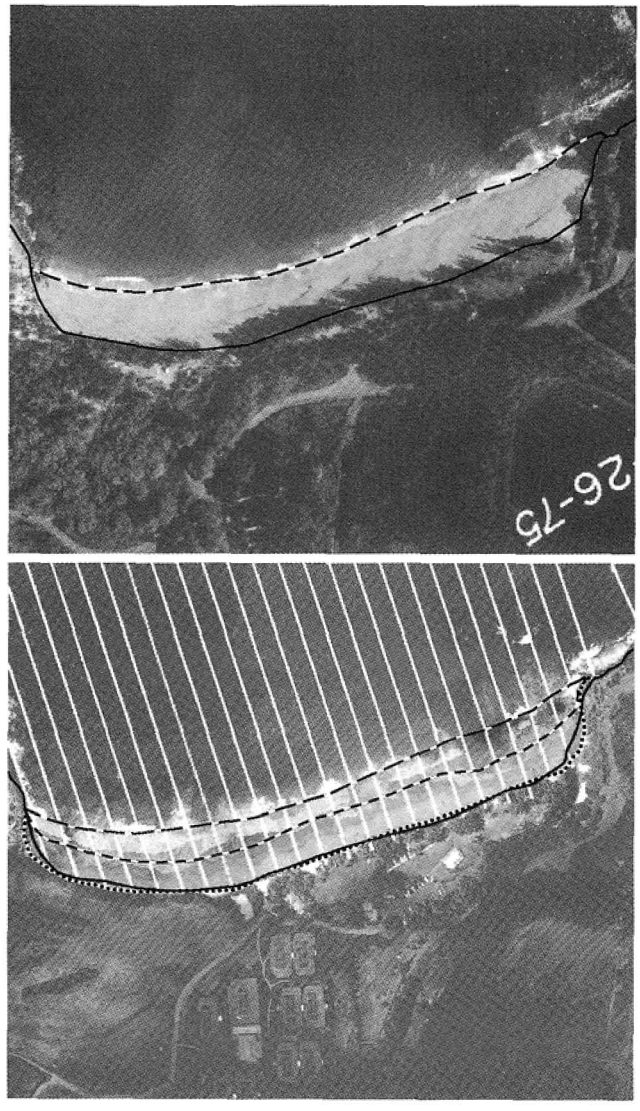

Figure 8. Top—1975 West Maui. Long Dashed—low water line; Solid—vegetation line. Bottom—1997 same beach. Long Dashed—1975 low water line; Short Dashed—1997 low water line; Dotted—1997 vegetation line; Solid—1975 vegetation line. Shore normal grid shows transect lines, spaced 20 m, which define locations where shoreline changes are measured.

change measurements. Data tables of shoreline position and date are collected for analysis at each transect. A vector representing the vegetation line is also collected contemporaneous to every low water vector in order to calculate changes in beach width through time (Figure 8).

We calculate two types of shoreline change rate: an end-point rate (EPR) and an annual erosion hazard rate (AEHR). The EPR is a simple measure of rate of change between the earliest shoreline, usually the 1900 or 1912 T-sheet and the 1997 or 2002 shoreline vectors. The AEHR is calculated using the slope of a straight-line fit to the reweighted (outliers removed) time series of shoreline positions using linear regression following CROWELL *et al.* (1997). The AEHR is then smoothed (averaged) in the alongshore direction using a weighted, five transect sliding filter. The filter calculates

Table 1. *Uncertainties related to positional and measurement errors*

Source	Magnitude
T-Sheets/H-Sheets	
1:5000	±3 m
1:10,000	±8.5 m
1:20,000	±10.4 m
Photo Measurement Uncertainty	
Onscreen Delineation	±3 m
RMS Orthorectification (includes pixel size and DEM contour interval)	±1.75 m (0.5–3 m)
Photo Positional Uncertainty	
Tide Stage	±3.0 m
Seasonal Variability	±8.6 m (5–20 m)
TOTAL UNCERTAINTY (U_t see text)	±14.25 m (for 1:20,000 T-sheet)
ANNUALIZED UNCERTAINTY (97 yr)	±0.14 m/yr

the average rate on five adjacent transects that are nominally weighted (1,3,5,3,1) and applies the average to the middle transect. The filter then slides to the next adjacent transect and applies the same procedure. This continues in the alongshore direction until a barrier to alongshore sediment movement is encountered such as a headland or a groin. The filter starts anew on the other side of such a barrier. The AEHR's reported here have been smoothed using this technique.

Uncertainty

Several sources of uncertainty (Table 1) impact the accuracy of historical shoreline positions and the final shoreline change rates. We define two types of uncertainty: positional uncertainty and measurement uncertainty.

Positional uncertainty is related to all features and phenomena that reduce the exactitude of defining the true shoreline position in a given year. These uncertainties mostly center on the nature of shoreline position at the time the aerial photo was collected. Influences on position include the stage of tide, the recent incidence of storms and the seasonal state of the beach. Each of these has been quantified as an uncertainty.

The uncertainty related to the tide stage is quantified through several field measurements of the shifting position of the low water mark across a spring tidal cycle. We measured this quantity at several locations and calculated a mean tidal uncertainty of 3.0 m for Maui Island. The seasonal uncertainty is defined as the difference in the low water position as measured in a winter 1988 aerial photograph compared to a summer 1987 aerial photograph of the same coast. These photos are available for almost all Maui study sites (Kuau, North Shore not available) and a measurement is calculated for every beach in the study. The mean seasonal uncertainty is 8.6 m and ranges from a single extreme measurement of 20 m to a minimum of 3 m. We also reiterate that the LMS procedure effectively removes extreme shorelines that fall off trend due to storm or tsunami impacts, seasonal processes, and human impacts so that the effect of these uncertainties significantly altering an erosion rate is unlikely.

The measurement uncertainty is related to operator-based manipulation of the map and photo products. For T-sheets, we adopt National Map Accuracy Standards that provide a measure of both position and measurement uncertainties. For photos, measurement uncertainty is related to the orthorectification process and onscreen delineation of the shoreline reference feature. The RMS report relates to orthorectification accuracy. The RMS values are measures of the misfit between points on a photo and established GCP's. RMS uncertainties range from 0.5 to 3 m. This also includes uncertainties related to photo pixel size (0.3–0.5 m) and DEM contour interval (10 m). The uncertainty related to onscreen delineation of the low water mark is calculated as 3 m by repeat trials to test reproducibility.

These uncertainties are random and uncorrelated and may be represented by a single measure calculated by summing in quadrature (the square root of the sum of the squares). Hence, where T is the T-sheet uncertainty (10.4 m for 1:20,000), S is the seasonal positional uncertainty (8.6 m), t is the tidal stage uncertainty (3.0 m), RMS (average of 1.75 m) is the reported uncertainty due to orthorectification accuracy (includes pixel size and DEM uncertainties), and O is uncertainty due to onscreen delineation of the toe of the beach, then $U_t = \pm\sqrt{T^2 + S^2 + t^2 + RMS^2 + O^2}$. U_t is ±14.25 m. This uncertainty is annualized over the 97 year time span of the time series and equals 0.14 m/yr when 1:20,000 T-sheets are used. It is less for larger scale T-sheets.

Because the sources of uncertainty are random, uncorrelated and unbiased across the study regions, they can be absorbed into the confidence interval calculated by the linear regression model

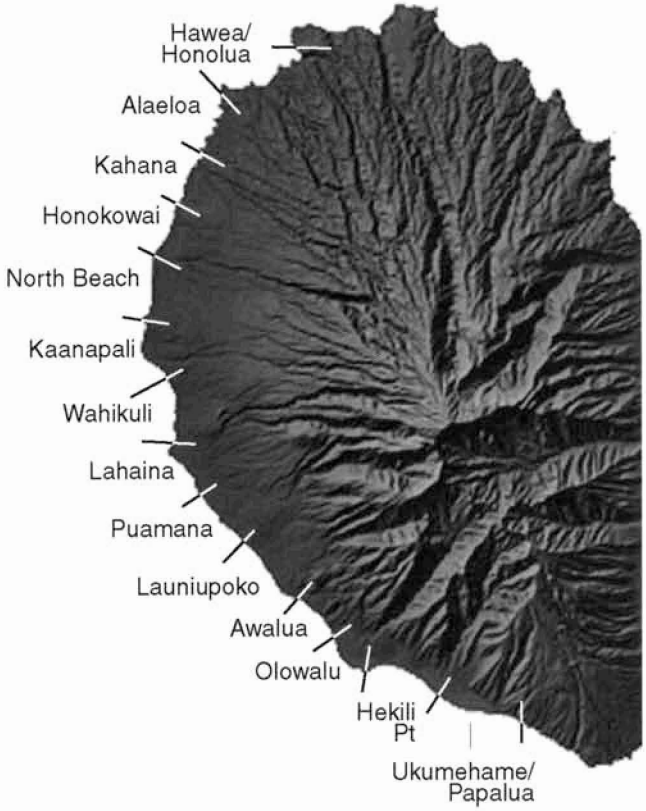

Figure 9. West Maui study area. Fourteen map areas covering 40 km.

used to determine the AEHR (NETER and WASSERMAN, 1974). The slope of the straight line fitted to historical shoreline data represents a model of the long-term trend of the shoreline. The residuals, or distances that individual shorelines are separated from the line, provide a measure of the goodness of fit. We calculate a model uncertainty associated with every annual erosion hazard rate providing a confidence interval at the 80th percentile (DOUGLASS *et al.* 1999).

RESULTS

West Maui

West Maui (Figure 9) extends from Ukumehame/Papalua in the south along a shore arcing clockwise to the north and ending at Honolua Bay. The coast has a generally western exposure with more southerly localities exposed to summer swell patterns as well as local seas generated by Kona storms and hurricanes. Northern localities are exposed to heavy winter swell. Central regions experience refracted energy related to both sets of swell patterns. In the lee of the West Maui Mountains, dominant trade winds generally blow either offshore or oblique to the shore.

The West Maui shore is characterized by heavily dissected highlands with watersheds that produce large alluvial fans during low sea-level stands. Once flooded by rising seas these platforms host the accretion of coral reefs often dominated by calcareous and coralline algae growth. Narrow, often sand depleted, beaches line the shoreline both where reefs are present as well as along open shore.

The smoothed average annual erosion rate (AEHR) for West Maui is 0.21 m/yr, the unsmoothed RLS rate is 0.22 ($\pm$ 0.13) m/yr, and the end point rate (EPR) is 0.21 m/yr. EVERSOLE (2002) calculated the historical sediment budget for Kaanapali and North Beach localities. He found erosion over the 48 yr period of study (1949–

Table 2. *Shoreline changes West Maui*

WEST MAUI Poster Area	Mean Rates (m/yr) AEHR	RLS	RLS Uncert.	Mean Shoreline Change Rate	EPR	Beach Width Change (%)	Beach Loss (km)
Hawea and Honolua	−0.12	−0.14	±0.14	−0.07	−0.26	−22%	0.00
Alaeloa	−0.29	−0.29	±0.17	−0.29	−0.29	−38%	0.08
Kahana	−0.21	−0.23	±0.18	−0.16	−0.27	−23%	0.58
Honokowai	−0.29	−0.29	±0.07	−0.28	−0.32	−36%	0.68
North Daanapali	−0.10	−0.10	±0.10	0.00	−0.09	−19%	0.00
Kaanapali	−0.20	−0.21	±0.11	−0.12	−0.19	−29%	0.10
Wahikuli	−0.20	−0.21	±0.13	−0.19	−0.20	−22%	0.96
Lahaina	−0.30	−0.32	±0.22	−0.12	−0.11	−26%	0.58
Puamana	−0.31	−0.35	±0.16	−0.13	−0.33	−29%	0.40
Launiupoko	−0.21	−0.22	±0.12	−0.17	−0.22	−34%	0.54
Awalua	−0.08	−0.09	±0.10	−0.05	−0.03	−22%	0.02
Olowalu	−0.13	−0.15	±0.09	−0.06	−0.04	−3%	0.00
Hekili Point	−0.21	−0.22	±0.07	−0.20	−0.25	−35%	0.36
Ukumehame and Papalaua	−0.31	−0.32	±0.15	−0.20	−0.41	−8%	0.18
TOTAL (average)	−0.21	−0.22	±0.13	−0.15	−0.21	−25%	4.48

1997) was mostly related to the episodic occurrence of Kona storms (early 1960's) and Hurricane Iniki (1992). The beach (430,000 m^3) experienced 220,000 m^3 of gross change over the period. Of this, 62 percent was attributed to storm erosion, another 33 percent was accreted, and 5 percent (a budget residual) was attributed to erosion due to relative sea-level rise. This residual erosion occurs in the form of slow but chronic shoreline recession equivalent to 73,000 m^3 over the ~50 year period.

Between 1949 and 1997 the average beach width narrowed by 25 percent over the West Maui region (Table 2). The greatest narrowing was centered on the Alaeloa (38 percent), Honokowai (36 percent), Launiupoko (34 percent), and Hekili Pt. (35 percent) map areas. Map areas with the greatest AEHR include Alaeola (0.29 m/yr), Honokowai (0.29 m/yr), Lahaina (0.30 m/yr), Puamana (0.31 m/yr), and Ukumehame/Papalua (0.31 m/yr). End point rates in most cases fall within 20 percent of the AEHRs. However at Hawea/Honolua, Lahaina, and Olowalu, the EPRs differ significantly from the AEHRs. Visual inspection of individual transects in these regions indicates the LMS technique identifies the T-sheet shoreline as an outlier point and in many cases calculates an erosion rate using more recent photo-based shorelines that produce a steeper regression line than if the T-sheet were included. However, the T-sheet shoreline clearly falls away from the trend defined by more recent photo shorelines.

Total beach loss for the region equals approximately 4.5 km. The worst cases of beach loss are found at Kahana (0.58 km), Honokowai (0.68 km), Wahikuli (0.96 km), Lahaina (0.58 km) and Launiupoko (0.54 km). The mean shoreline change rate at West Maui, including all transects (accreting, stable, and eroding) is −0.15 m/yr (eroding).

It is interesting to recognize that measures such as beach width changes, erosion rates, and beach loss each tend to be worse in different, rather than the same, areas. We speculate that these attributes may measure different phases of the same process (sand volume decrease through time) and so the map regions are in various stages of chronic sand volume loss. These stages might include: 1. increase of the AEHR if erosion is a relatively recent process; 2. increase of the EPR if erosion has been chronic over a long period; 3. decrease in beach width following chronic erosion; 4. threat to a highway or building; 5. beach loss due to armoring to protect a highway or building. The regions of Hawea/Honolua, North Kaanapali, Awalua, and Olowalu are the most stable of the region, yet still show a net erosional trend averaging 0.10 m/yr and average beach loss of 16.5 percent. Both these areas are notable for their lack of human impact and their retention of a fairly natural character.

Kihei Coastline

Kihei Coast (Figure 10) extends from Makena/BigBeach in the south along a linear shore that runs due north to Maalaea Bay and arcs sharply to the west in a fishhook ending at Maalaea Boat Harbor. The coast has a generally western expo-

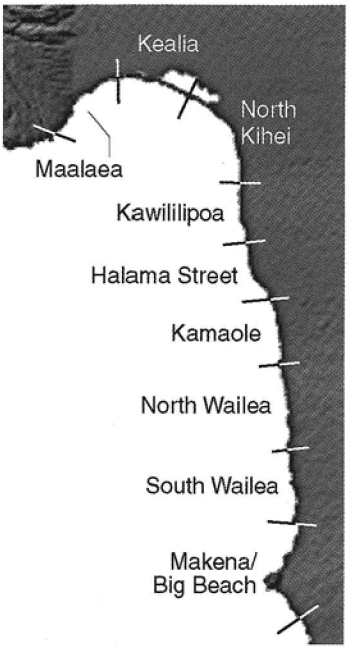

Figure 10. Kihei Coast study area. Nine map areas covering 27 km.

sure but sits in the wave shadow of Molokai, Lanai, and Kahoolawe and so mostly experiences significant swell energy from the south. Along the middle reach of the coast north swell energy does lead to seasonal changes in beach configuration. Local seas, generated by Kona storms and hurricanes, are a significant factor in the historical behavior of the shoreline. Because this shore sits in the lee of Haleakala Volcano, dominant trade winds generally blow either offshore (northern map areas) or strongly parallel to the shore and onshore influenced by diurnal heating of the volcanic uplands (central and southern map areas).

Kihei Coast is characterized by relatively young highlands with watersheds that lack heavily dissected valleys. The coastal plain is a flat, sand rich terrace with aquatic wetlands fronted by a calcareous coastal dune and a coral, calcareous algae, and coralline algae-dominated fringing reef in the central area. Map areas to the north and south host coral growth on the seafloor but lack true fringing reef. Narrow, often sand depleted, beaches line the fringing reef while generally wider, more sand-rich beaches are found to the south and north where human impact is absent.

The smoothed average annual erosion rate for Kihei is 0.29 m/yr, the RLS rate is 0.30 (± 0.17) m/yr, and the end point rate is 0.20 m/yr. The mean shoreline change rate for all transects (accreting, stable, and eroding) is −0.20 m/yr (eroding). ROONEY and FLETCHER (2000) calculate the historical sediment budget for the Kawililipoa, Halama Street, and Kamaole map areas. They found that between 1912 and 1949, the southern part experienced erosion while the northern portion accreted. The most severe erosion occurred along the southern portion of Kalama Beach Park, averaging 1.8 m/yr. In successively later years the focus of erosion migrated to the north end of the Halama Street area while Kawililipoa continued accreting. A shift from net accretion to erosion across the entire area started around 1975. Low rates of net sediment transport since 1975 are primarily due to sediment impoundment by coastal armoring. They identify the combined influence of coastal armoring and a series of strong Kona storms associated with an earlier phase of the Pacific Decadal Oscillation that transported sediment to the north, opposite the present regime, as being responsible for recent erosion trends.

Between 1949 and 1997 the average beach width on the Kihei coast narrowed by 19 percent (Table 3). The greatest narrowing was centered at Halama Street (34 percent). North Kihei (28 percent) and North Wailea (30 percent) map areas experienced moderate narrowing of about one third. Map areas with the greatest AEHR include Kawililipoa (0.32 m/yr), Halama Street (0.46 m/yr), and North Wailea (0.32 m/yr). EPRs in four map areas differ significantly from AEHRs (Maalaea Harbor, Halama Street, Kamaole, and North Wailea). However the remainder also show significant variation. As in the West Maui region, the linear regression technique that calculates the AEHR identifies the T-sheet shoreline as an outlier point in many of these cases. At South Wailea and Makena the available T-sheet was found to be significantly distorted and so was not used in calculating AEHR values. At Kawililipoa, the long period of sediment accumulation is reflected in an EPR that shows accretion (0.34 m/yr), while the AEHR reflects a more recent erosion trend (0.32 m/yr). Total beach loss on the Kihei coast is 2.8 km.

North Shore

North Shore reaches from Waihee Point in the west along a gently curving embayed shore that

Table 3. *Shoreline changes Kihei Coast*

KIHIE COAST Poster Area	Mean Rates (m/yr) AEHRs	RLS	RLS Uncert	Mean Shoreline Change Rates	EPRs	Beach Width Change (%)	Beach Loss (km)
Maalaea Harbor	−0.27	−0.28	±0.14	−0.27	−0.52	−11%	0.68
Kealia Pond	−0.21	−0.22	±0.12	−0.18	−0.25	5%	0.00
North Kihei	−0.28	−0.28	±0.10	−0.25	−0.22	−28%	0.14
Kawililipoa	−0.32	−0.30	±0.19	0.12	0.34	−21%	0.10
Halama Street	−0.46	−0.49	±0.19	−0.17	−0.23	−34%	1.56
Kamaole	−0.21	−0.27	±0.36	−0.23	−0.30	−17%	0.14
North Wailea	−0.32	−0.34	±0.19	−0.32	−0.22	−30%	0.00
South Wailea	−0.29	−0.29	±0.12	−0.28	−0.21	−17%	0.06
Big Beach/Makena	−0.22	−0.24	±0.13	−0.19	−0.23	−10%	0.12
TOTAL (average)	−0.29	−0.30	±0.17	−0.20	−0.20	−19%	2.80

extends to the east ending at Kuau (Figure 11). A major cultural feature is Kahului Deep Draft Harbor. The coast has a generally northern exposure and receives seasonal winter swell from the North Pacific as well as the ever-present trade wind seas that persist throughout 75 percent of the year. Trades in general blow directly onshore. The shoreline is dominated in the west by cobble and sand beach, in the central region by sand beach interrupted by shoreline structures, and in the east by sand beach interspersed with rocky headlands.

North Shore region is characterized by heavy rainfall and run off from the dissected watersheds of the West Maui highlands in northern map areas (Waihee, Waiehu). Kahului area marks the transition to low lying hinterlands (Maui saddle region) characterized by a sand-rich coastal plain with wetlands and frontal sand dunes (Kahului, Kanaha, Spreckelsville, and Baldwin map areas). A crustose algae-dominated fringing reef is found offshore of both northern and central map areas but it is relatively deep close to shore in many map areas and allows for trade wind waves 0.5 to 1.5 m in height incident to the shoreline. A steep coastal plain associated with the rising slopes of Haleakala volcano marks eastern portions of the Baldwin and Kuau map areas. Consequently, short, embayed pocket beaches and narrow perched beaches on low elevation rocky terraces characterize the coastline.

Although no specific research has been published regarding the causes of erosion patterns on the North Shore, local residents report that extensive run-up associated a large tsunami last century caused extensive shoreline recession. This is consistent with our observations of a large offset between the T-sheet shoreline of 1912 and the earliest photographic shoreline in 1949. Several rocky headlands to the east of Baldwin Beach Park in the vicinity of Paia Beach Park are low lying and record a dramatic landward shift in the shoreline during this period. The 1946 tsunami, which killed over 100 people throughout Hawaii, occurred im-

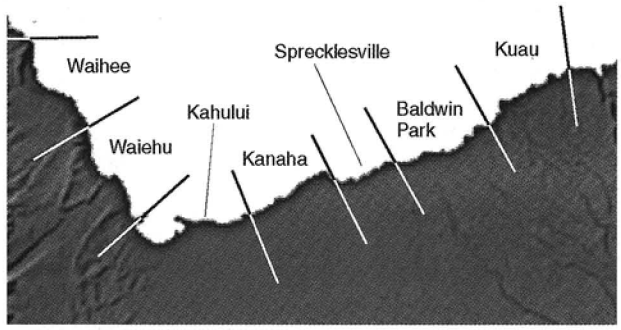

Figure 11. North Shore study area. Seven map areas covering 22 km.

Table 4. *Shoreline changes North Shore*

NORTH SHORE Poster Area	Mean Rates (m/yr) AEHRs	RLS	RLS Uncert.	Mean Shoreline Change Rates	EPRs	Beach Width Change (%)	Beach Loss (km)
Waihee	−0.26	−0.26	±0.09	−0.19	−0.04	−17%	0.00
Waiehu	−0.18	−0.19	±0.09	−0.11	−0.08	−32%	0.12
Kahului Harbor	−0.47	−0.49	±0.12	−0.37	−0.22	−20%	0.30
Kanaha	−0.45	−0.45	±0.16	−0.03	−0.26	25%	0.12
Sprecklesville	−0.53	−0.53	±0.24	−0.53	−0.47	−2%	0.12
Baldwin Park	−0.50	−0.51	±0.31	−0.50	−0.68	−7%	0.08
Kuau	−0.31	−0.32	±0.23	−0.30	−0.28	−2%	0.06
TOTAL (average)	−0.38	−0.39	±0.18	−0.29	−0.29	−15%	0.80

mediately prior to the 1949 photoseries and is a likely candidate for causing the observed recession. Additionally, widespread sand mining to furnish lime for agriculture also took place along the North Shore. The limekiln at Baldwin Beach Park still stands today as testimony to decades of this damaging practice.

The smoothed average annual erosion rate for the North Shore is 0.38 m/yr, the RLS is 0.39 (± 0.18) m/yr, and the end point rate is 0.29 m/yr. The mean shoreline change rate for all transects (accreting, stable, and eroding) is −0.29 m/yr (eroding). Between 1949 and 1997, the average beach width on the North Shore narrowed by 15% (Table 4). The greatest narrowing was centered on the Waiehu area (32 percent). At Kanaha map area the average beach width increased over the study period by 25 percent. The greatest AEHR is found in the Spreckelsville map area (0.53 m/yr). The Kahului Harbor area experienced 0.47 m/yr erosion, while Kanaha eroded at approximately 0.45 m/yr. Baldwin map area also experienced pronounced erosion at 0.50 m/yr. EPRs differ from AEHRs significantly on the North Shore at nearly all map areas. This is due to the rejection of the T-sheet shoreline as an outlier point by the reweighted linear regression. Total beach loss for the North Shore is 0.80 km.

DISCUSSION

For the first time in the state of Hawaii, a highly detailed and accurate analysis of historical shoreline migration has been completed for all the significant sandy shoreline on an entire island. Making use of all available maps and aerial photos meeting stringent precision and accuracy guidelines, the historical landward and seaward boundaries of the beach have been digitized and their movement documented at an alongshore spacing of 20 m for the significant sandy shoreline of Maui. The resulting history of shoreline change has been modeled using a reweighted least squares linear regression to determine long-term trends and rates of chronic shoreline change free from the influence of anomalous positions of the coast (e.g., storm shorelines).

Although the process of historical shoreline analysis has become digitally-based and software dependent, the role of professional judgment remains important. While the use of T-sheets enhances the final product, their use is improved by including some form of testing or visual inspection to ascertain the validity of the shoreline they provide.

Special effort was made to define the uncertainties (errors) associated with our methodology. Important to this analysis was a network of beach profile monitoring stations established in an earlier research project. These monitoring stations provided accurate measurements of the horizontal offset between the high water mark that is mapped on T-sheets and the low water position used as the shoreline change reference feature. The offset is an average five year value taken from the nearest appropriate profile location so that it represents seasonal, wave state, and tidal influences on the offset. Monitoring stations also acted as a reference source when questions arose regarding shoreline features in the onscreen digitizing process. Another source of uncertainty is the seasonal state of the beach. Aerial photographs covering the entire field area from winter 1987 and summer 1986 were employed to document the shift in shoreline position and provided site-specific measurements of seasonal uncertainty.

The size and scope of the project and the lack of

a reliable event history made it necessary to establish a methodology of determining the rate of shoreline change that was sufficiently robust to handle the multiplicity of coastal processes and histories that characterize the Maui coast as well as maximize the information yield to resource managers. Hence, we provide two rates of change each of which has their advantages and disadvantages. The EPR describes the longest possible trend in shoreline change and minimizes the potential for inaccuracies due to short-term shoreline fluctuations. However, either (or both) of the two shorelines used to determine the EPR might itself be the product of a short-term fluctuation. Additionally, EPR relies upon a T-sheet shoreline that is less accurate than a photogrammetrically corrected shoreline. The AEHR utilizes a reweighted linear regression to determine a trend in shoreline change. Calculating a reweighted dataset is a robust method of minimizing variability due to short-term shoreline fluctuations. Additionally, by modeling the entire dataset, the linear regression method is more sensitive to significant shifts in historical patterns of change as well as more representative of all shoreline positions. However, the AEHR may ignore recent accelerations in shoreline erosion due to increased human impacts to coastal sediment budgets. The proliferation of shoreline armoring and the sand impoundment it causes, as well as a reputed history of sand mining, have significantly decreased available sand sources along all Maui beaches. This, along with the inferred role of relative sea-level rise as an agent of change, has lead to the complete loss of many beaches and narrowing of others. In many cases, the AEHR does not reflect accelerated erosion rates that caused these losses. As such, coastal managers may not be fully informed regarding impending beach loss or the full hazard incident to landowners. That is, there may be cases where the true erosion rate is underestimated.

Shoreline Change Trends

The mean, island-wide rate of shoreline change using all transects (eroding, stable, and accreting) is 0.21 m/yr. The mean island-wide rate of erosion using the smoothed AEHR method (0.29 m/yr, erosion) differs somewhat from the mean EPR rate (0.24 m/yr). Both types of erosion rates on Maui's North Shore are substantially higher than those on the Kihei and West Maui sides of the island. Island wide beach width decreased 19 percent over the period 1949 to 1997/2002. We note that although erosion rates are higher, beach widths on the North Shore have decreased significantly less than those on Kihei and West Maui shores.

Research efforts conducted in parallel with the mapping effort along the Kihei coast (southwest Maui) suggest that much of the decadal to century scale shoreline sediment dynamics are driven by variations in the Pacific Decadal Oscillation (PDO). Positive or El Nino-like phases of the PDO appear to inhibit Kona storm activity, resulting in predominantly southward, trade-wind driven net longshore sediment transport (NLST). During negative PDO phases, occasional severe Kona storms induce high rates of northward NLST. Analysis of the historical pattern of erosion and accretion in Kaanapali on the west coast of Maui reveals that the area is subject to long periods of mild erosion and accretion punctuated by severe erosional events related to short-period Kona storms and hurricanes. Like Kona storms, hurricane activity in Hawaii is modulated by the PDO and the El Nino/Southern Oscillation (ENSO). However, during positive phases of the PDO (and negative ENSO phases), there is a tendency for enhanced hurricane but reduced Kona storm activity in the islands. Although not necessarily representative of all sandy shoreline areas on this or other islands, results suggest that interannual to century scale shoreline sediment dynamics are strongly influenced by PDO and ENSO-related storm variability. Other factors, such as human impacts, are likely to be important as well.

Human impacts are often more difficult to quantify. However, the incidence of such damaging practices such as impounding coastal plain sand with armoring, directly removing beach sand for lime production, and clearing drainage canals that have filled with beach sand are widespread along the Maui shoreline, and it is unlikely that the cumulative impact would be insignificant. These are likely to be important given the slow rate of sediment production associated with fringing reefs (HARNEY *et al.*, 1999; EVERSOLE, 2002). Radiocarbon dates of carbonate sands from reef top and shoreline environments reveal their fossil origin (ca. 1500 to 4000 years Before Present) even on accreting beaches. As shown by ROONEY (2001), NORCROSS *et al.* (2002) and EVERSOLE (2002), Hawaiian beaches tend to be dominated by longshore sediment transport rather than cross-shore transport. This indicates that beaches are not sustained by prolific delivery of offshore sands. Rather they

are likely the eroding front of an extensive deposit of fossil beach and dune sands that blanket the coastal plain. This deposit dates from the late middle Holocene sea-level highstand which stood some 2 m higher than present (HARNEY *et al.*, 1999; FLETCHER and JONES, 1996) and was a time of enhanced sediment production on the fringing reef surface. The sediment reservoir characterizing most Hawaiian beaches is not actively fed by offshore delivery, it dates from a former time of higher production under conditions that do not exist today, and the largest and most actively accessed sediment stores lie immediately landward of beaches on the coastal plain. Given these conditions, it seems reasonable to infer that sand impoundment and sand mining (including drainage clearing) act to destabilize Maui beaches rendering them vulnerable to storm impacts governed by regional-scale climatic processes.

CONCLUSIONS

Tourism provides over 60 percent of jobs in Hawaii, and beaches are a major reason why visitors come to the islands. The problem of coastal erosion is a source of widespread concern because of threats to abutting private lands and loss of beach resources. A combination of NOAA T-sheets and large-scale, orthorectified vertical aerial photographs with ground resolution of 0.3–0.5 m were used to determine historical shoreline positions. This dataset is characterized by:

1. Statistically significant long-term trends (uncertainties are typically less than trends);
2. Measurements representing long-term shoreline change (influence of extreme events is minimized);
3. High-resolution historical shoreline positions (movement of the low water position is sensitive to changes in beach volume);
4. High precision data sources (photographs are orthorectified and positional uncertainties are tracked); and,
5. High spatial density (every beach in the study area is described with an alongshore sampling of 20 m).

T-sheets, provided by the NOAA Coastal Services Center at national map accuracy standards, considerably enhanced the temporal and spatial coverage of the study as well as the accuracy, precision and significance of the resulting database. Triangulation stations on georectified survey sheets were tested against modern orthorectified photomosaics, a misfit greater than national map accuracy standards lead to rejection of the T-sheet shoreline. On some maps passing these tests, shoreline vectors were corrected using stable shoreline features to improve their fit.

Because the position of mllw is the most appropriate reference feature for documenting historical shoreline movement in Hawaii, T-sheet shorelines representing the high water mark were horizontally migrated to match the contemporaneous position of mllw. This was achieved using spatial models derived from a five-year series of beach profiles. Time series of shoreline positions were evaluated using least median of squares regression to remove or reduce the influence of outliers produced by storms, seasonal swell, or other temporary state not related to long-term trend. Rates of shoreline change using the reweighted data were calculated using end point and linear regression methodologies. Overall, the methodology yields measurement and position uncertainties less than or equal to 0.14 m/yr. However, because these are random, uncorrelated, and unbiased, the linear regression model absorbs all positional and measurement uncertainties such that the final error is reported as the 80th percentile confidence interval of the regression procedure.

The AEHR and EPR for West Maui both average approximately 0.2 m/yr. Between 1949 and 1997 the average beach width narrowed by 25 percent. Total beach loss for the region equals approximately 4.5 km. The worst cases of beach loss are found at Kahana (0.58 km), Honokowai (0.68 km), Wahikuli (0.96 km), Lahaina (0.58 km) and Launiupoko (0.54 km).

The AEHR for Kihei is approximately 0.3 m/yr and the EPR is 0.2 m/yr. Between 1949 and 1997 the average beach width on the Kihei coast narrowed by 19 percent. The greatest narrowing was centered at Halama Street (34 percent). The North Kihei (28 percent), and North Wailea (30 percent) map areas experienced moderate narrowing of about one third. Map areas with the greatest AEHR include Kawililipoa (0.32 m/yr), Halama Street (0.46 m/yr), and North Wailae (0.32 m/yr) and South Wailea (0.29 m/yr). A shift from net accretion to erosion across the entire area started around 1975. Total beach loss on the Kihei coast is 2.8 km.

The AEHR for the North Shore is about 0.4 m/yr and the EPR is about 0.3 m/yr. Between 1949 and 1997 the average beach width on the North

Shore narrowed by 15 percent. The greatest narrowing was centered at Waiehu (32 percent). Total beach loss for the North Shore is 0.8 km.

The mean, island-wide EPR is 0.24 m/yr and the AEHR is 0.29 m/yr. Both types of erosion rates on Maui's North Shore are significantly higher than those on the Kihei and West Maui coasts. Island wide changes in beach width show a 19 percent decrease over the period 1949 to 1997/2002. Although erosion rates are higher, beach widths on the North Shore have decreased less than those on Kihei and West Maui shores. Island-wide, over 8 km of beach has been lost since 1949.

Several natural and anthropogenic causes of erosion are known on Maui including storms, sediment impoundment, sand mining and relative sea-level rise. Data presented in this study document chronic erosion. Actual erosion on any given beach may be greater than documented as the result of episodic erosion associated with seasonal and other short-term phenomena. Joined with chronic erosion this can lead to accelerated rates of shoreline change.

ACKNOWLEDGEMENTS

Funding for this study was made available by the U.S. Geological Survey, the Hawaii Sea Grant College, the NOAA Coastal Services Center, Maui County, and the Hawaii Coastal Zone Management Program. We gratefully acknowledge advice and assistance provided by Mike Rink (NOAA); Daren Suzuki, Matt Niles (Maui Co.); Kevin Bodge (Olsen Engineering, Inc.); Cheryl Hapke, Ann Gibbs, Tom Reiss and Abby Sallenger (USGS); Zoe Norcross, and Dolan Eversole (UH Sea Grant); Mary Engels, Ayesha Genz, Rob Mullane, Ole Kaven, and Eden Fierstein (UH Coastal Geology Group). Editorial suggestions by Mark Byrnes and James O'Connell greatly improved the scope and content of the manuscript.

LITERATURE CITED

ANDERS, F.J. and BYRNES, M.R., 1991. Accuracy of shoreline change rates as determined from maps and aerial photographs, *Shore and Beach,* January, 17–26.

BAUER, B.O. and ALLEN, J.R., 1995. Beach steps: an evolutionary perspective. *Marine Geology,* 123, 143–166.

CALHOUN, R.S. and FLETCHER C.H., 1995. Late Holocene coastal plain stratigraphy and sea-level history at Hanalei, Kauai, Hawaiian Islands. *Quaternary Research,* 45, 47–58.

CROWELL, M.; DOUGLAS, B.C., and LEATHERMAN, S.P., 1997. On forecasting future shoreline positions: A test of algorithms. *Journal of Coastal Research,* 13 (4), 1245–1255.

CROWELL, M.; LEATHERMAN, S.P., and BUCKLEY, M. K., 1993. Shoreline change rate analysis: Long term versus shore term data. *Shore and Beach,* 61 (2), 13–20.

CROWELL, M.; LEATHERMAN, S.P., and BUCKLEY, M.K., 1991. Historical shoreline change: Error analysis and mapping accuracy. *Journal of Coastal Research,* 7 (3), 839–852.

DAIL, H.J.; MERRIFIELD, M.A., and BEVIS, M., 2000. Steep beach morphology changes due to energetic wave forcing. *Marine Geology,* 162, 443–458.

DANIELS, R.C. and HUXFORD, R.H., 2001. An error assessment of vector data derived from scanned National Ocean service topographic sheets. *Journal of Coastal Research,* 17 (3), 611–619.

DOUGLAS, B.C. AND CROWELL, M., 2000. Long-term prediction and error propagation. *Journal of Coastal Research,* 16 (1), 145–152.

DOUGLASS, S.L.; SANCHEZ, T.A., and JENKINS, S., 1999. Mapping erosion hazard areas in Baldwin County, Alabama and the use of confidence intervals in shoreline change analysis. *Journal of Coastal Research,* Special Issue No. 28, 95–105.

ELLIS, M.Y. (ED.), 1978. Coastal Mapping Handbook, U.S. Department of the Interior, Geological Survey; U.S. Department of Commerce, National Ocean Survey; U.S. Government Printing Office, Washington, D.C., 199p.

EVERSOLE, D., 2002. *Large scale beach change, Kaanapali, Hawaii.* M.S. Thesis, University of Hawaii, 96p.

FLETCHER, C.H. and JONES, A.T., 1996. Sea-level highstand recorded in Holocene shoreline deposits on Oahu, Hawaii. *Journal of Sedimentary Research,* 66 (3), 632–641.

FLETCHER, C.H.; MULLANE, R.A., and RICHMOND, B.R., 1997. Beach loss along armored shorelines on Oahu, Hawaiian Islands. *Journal of Coastal Research,* 13 (1), 209–215.

FLETCHER, C.H. and LEMMO, S.J., 1999. Hawaii's emergent coastal erosion management program. *Shore and Beach,* 67 (4), 15–20.

FLETCHER, C.H.; GROSSMAN, E.E.; RICHMOND, B.M., and GIBBS, A.E., 2002. Atlas of Natural Hazards in the Hawaiian Coastal Zone, U.S. Geological Survey, Geologic Investigation Series, I-2761, http://geopubs.wr.usgs.gov/I-map/i2761/, Federal Center, Denver CO.

GIBBS, A.E.; RICHMOND, B.M.; FLETCHER, C.H., and HILMAN, K.P., 2002. Hawaii Beach Monitoring Program, U.S. Geological Survey, Open File Report 01-308, v.1.0, http://geopubs.wr.usgs.gov/open-file/of01-308, Federal Center, Denver CO.

GROSSMAN, E.E. and FLETCHER, C.H., 1998. Sea level 3500 years ago on the Northern Main Hawaiian Islands. *Geology,* 26 (4), 363–366.

HARNEY, J.N.; GROSSMAN, E.E.; RICHMOND, B.M., and FLETCHER, C.H., 1999. Age and composition of carbonate shoreface sediments, Kailua Bay, Oahu, Hawaii. *Coral Reefs,* 19, 141–154.

HARNEY, J.N., and FLETCHER, C.H., in press. A carbonate budget for a fringing reef, Kailua Bay, Hawaii. *Journal of Sedimentary Research,* (10/2002).

HONEYCUTT, M.G.; CROWELL, M., and DOUGLASS, B.C.,

2001. Shoreline position forecasting: Impact of Storms, rate calculation methodologies and temporal scales. *Journal of Coastal Research,* 17 (3), 721–730.

NATIONAL ACADEMY OF SCIENCES, 1990. Managing Coastal Erosion. National Research Council, Committee on Coastal Erosion Zone Management, National Academy Press, Washington, 182p.

NETER, J. and WASSERMAN, W., 1974. Applied Linear Statistical Models. R.D., Irwin, Inc., Homewood, Ill. 167p.

NORCROSS, Z.M.; FLETCHER, C.H., and MERRIFIELD, M., 2002. Annual and interannual changes on a reef-fringed pocket beach: Kailua Bay, Hawaii. *Marine Geology,* 3203, 1–28.

ROONEY, J.J.B., 2001. A century of shoreline change along the Kihei coast of Maui, Hawaii. Ph.D. Dissertation, University of Hawaii, 96p.

ROONEY, J.J.B. and FLETCHER, C.H., 2000. A high resolution, digital, aerial photogrammetric analysis of historical shoreline change and net sediment transport along the Kihei Coast of Maui, Hawaii. *In: Proceedings of Thirteenth Annual National Conference on Beach Preservation Technology,* Feb. 2–4, Melbourne, FL.

ROUSSEEUW, P.J., 1990. Robust estimation and identifying outliers, *In, H.M. Wadsworth,* (Ed.), *Handbook of Statistical Methods for Engineers and Scientists,* McGraw-Hill Pub. Co., New York, NY, 16.1–16.24.